Pergamon

Int. J. Heat Mass Transfer. Vol. 38, No. 11, pp. 2029–2037, 1995

0017-9310/95 $9.50+0.00

0017-9310(94)00317-3

Calibration of a photographic method for imaging mass transfer in aqueous solutions

A. DASGUPTA, P. GUENARD, S. M. ANDERSON, J. S. KARSNITZ and J. S. ULTMAN†

Department of Chemical Engineering, Pennsylvania State University, University, PA 16802 U.S.A.

and

K. T. MORGAN

Chemical Industry Institute of Toxicology, Research Triangle Park, NC 27709, U.S.A.

(*Received* 28 *October* 1992 *and in final form* 23 *September* 1994)

Abstract—We previously described a method utilizing the flow of developer solution over an exposed photographic film for imaging mass uptake patterns at solid surfaces. We have now formulated a calibration equation that converts optical density of the developed black-and-white film to the local mass transfer coefficient. This equation was evaluated with measurements of mass transfer at the surface of a spinning disk and in the entry region of a straight tube. The product of developer dilution and development time dictated the broadest range of measurable mass transfer coefficient values and had an optimum value of approximately 1.0 min.

INTRODUCTION

Mass transport in complex velocity fields has long been a subject of interest. Yet, few methods exist for measuring the distribution of solute flux under different flow conditions, and these methods all have important limitations. Electrochemical probes, which measure the current generated by a diffusion-limited electron transfer reaction, do not provide good spatial resolution [1]. Profilometric methods, which are based on the direct loss of pure solid coatings [2] or the loss of solute from swollen polymer coatings [3], yield patterns of surface erosion that can provide excellent spatial resolution. However, the interpretation of these surface patterns requires tedious and/or sophisticated measurement strategies. In response to the need for an improved method of visualizing mass transfer patterns, we are investigating a photographic technique which is simple and inexpensive to use, and which can utilize commonly-found video image analysis equipment for data processing.

The thin emulsion that coats a photographic film contains a large number of minute 'grains' of transparent silver halide crystals suspended in gelatin. When a photograph is taken, a few atoms of silver halide are reduced to metallic silver in each of the grains that is exposed to light. To develop this imperceptible 'latent image', the film is treated with a chemical reducing agent that forms additional silver atoms within the exposed grains, thereby rendering them opaque [4]. In the photographic method we have conceived, a black-and-white film is totally exposed to light, attached to a test surface, and then subjected to the flow of aqueous developer solution. Since chemical reduction of the silver halide is fast, the convective-diffusion of developer to the emulsion surface strongly influences the local increase in opacity of the film. Therefore, the image appearing on the fixed emulsion serves as a permanent record of the spatial distribution of mass uptake.

In a previous study, we applied the photographic method to flow over a backward facing step, a right circular cylinder and a square resting on the bottom of a liquid flow channel [5]. Though the images we obtained were quantified by optical density measurements, the absence of a functional relationship between OD and mass transfer coefficient limited the usefulness of the data. The purposes of the current research were: to formulate a calibration equation for converting OD measurements into k_c values; to use a spinning disk experiment for estimating unknown parameters in the calibration equation; and to verify the calibration equation by applying it to entrance flow in a straight tube.

MATHEMATICAL MODELING

Reaction kinetics of film development

A silver bromide-based film and a hydroquinone-based developer solution were selected for this research. In that case, film development occurs by a multistep mechanism in which a doubly-charged

†Author to whom correspondence should be addressed.

NOMENCLATURE

C_H, C_{Ho}, C_{Hs} concentrations of hydroquinone in the emulsion, diluted developer and stock developer [kmol m^{-3}]

C_{So}, C_S concentration of silver in the emulsion, initially (due to the latent image) and at some time later [kmol m^{-3}]

C_{SBo}, C_{SB} concentration of silver bromide in the emulsion, initially and at some time later [kmol m^{-3}]

D_H effective binary diffusion coefficient of hydroquinone in developer solution [m^2 s^{-1}]

$k_c, (k_c)_{ref}$ mass transfer coefficient on the film surface at an arbitrary point and at a reference point [m^2 s^{-1}]

k'_r, k_r lumped parameter rate constants for reaction I and reaction II [s^{-1}]

k_I, k_{II} rate constants for reaction I [m^6/kmol^2/s] and reaction II [m^3 kmol^{-1} s^{-1}]

L thickness of the emulsion layer [m]

n the stoichiometric ratio between the number of hydroquinone molecules that are reacted and the number of silver cations that are reduced.

OD, OD_0, OD_∞ optical density of exposed film that has been partially developed, undeveloped and completely developed.

$OD', (OD')_{ref}$ normalized optical density on the film, equation (11), at an arbitrary and at a reference point

r_H, r_{SB} rate of chemical depletion of hydroquinone and of silver bromide [kmol m^{-3} s^{-1}]

R tube radius [m]

Re Reynolds number, the ratio of the volumetric liquid flow rate per unit channel width to the kinematic viscosity

t development time [s]

u average velocity of liquid through a straight tube [m s^{-1}]

X developer dilution factor

z, z_{ref} axial distance from leading edge of film at an arbitrary point and at a reference point [m].

Greek symbols

α optical extinction coefficient [m^2 kmol^{-1}]

β lumped calibration parameter [m s^{-1}]

ν kinematic viscosity [m^2 s^{-1}]

λ equilibrium ratio of hydroquinone concentration between developer solution and emulsion

ω rotational frequency [rad s^{-1}].

hydroquinone anion first reacts with one silver cation to form a singly-charged semiquinone free radial and a reduced silver atom. Because sodium sulfite is also present in the developer, the semiquinone reduces additional silver cations, producing hydroquinone monosulphonate and hydroquinone disulphonate as reaction byproducts [6]. The rate of these reactions may be enhanced by silver atoms, and it is this autocatalytic property that accounts for the spatial specificity and speed of latent image development [7].

In modelling these complex kinetics, we assumed that the autocatalytic production of the semiquinone radical is rate-controlling and the reaction is first-order with respect to hydroquinonone, silver bromide, and the reduced silver concentrations. In that case, the rate of depletion of silver bromide per unit volume of emulsion is given by (reaction I)

$$r_{SB} = k_I C_H C_{SB} C_S. \tag{1a}$$

As an alternative scenario, we considered the production of semiquinone under noncatalytic conditions (reaction II)

$$r_{SB} = k_{II} C_H C_{SB}. \tag{1b}$$

We also assumed that the emulsion layer is so thin that it is well-mixed by diffusion. This implies that C_{SB}, C_S and C_H do not vary with depth into the emulsion.

A choice between the alternative rate expressions, (1a) and (1b), will be based on an experiment in which the emulsion is submerged in a well-mixed developer solution. In that case, the hydroquinone concentration in direct contact with the emulsion surface is the same as the bulk concentration of hydroquinone in developer solution. It is also assumed that the distribution of hydroquinone concentration between the developer and the emulsion is prescribed by a constant equilibrium ratio so that

$$C_{Ho} = \lambda C_H. \tag{2}$$

A material balance on the silver bromide in the emulsion yields

$$d(C_{SB})/dt = -r_{SB}. \tag{3}$$

Since neither silver bromide nor reduced silver can leave the emulsion, an overall material balance yields

$$C_S = (C_{SBo} + C_{So}) - C_{SB}. \tag{4}$$

If there is a sufficient excess of hydroquinone in the developer, then the decrease in C_{Ho} due to reaction in the emulsion will be negligible and equations (1)–(4) can be solved to obtain

$$C_{SB}/(C_{SBo}+C_{So}) = \{1+(C_{So}/C_{SBo}) \times \exp[(k_I(C_{SBo}+C_{So})/\lambda)(C_{Ho}t)]\}^{-1} \quad (5a)$$

for reaction I and

$$C_{SB}/C_{SBo} = \exp[-(k_{II}/\lambda)(C_{Ho}t)] \quad (5b)$$

for reaction II.

To compare these predictions to experimental data, the silver bromide concentrations must be related to the optical density of the emulsion. Optical density can be written in terms of silver concentration in the emulsion by using the Beer–Lambert law of light transmission

$$OD = OD_o + (\alpha L)(C_S - C_{So}). \quad (6)$$

Recognizing that a maximum optical density, OD_∞, occurs when all the silver bromide has been reduced to silver, equations (4) and (6) lead to

$$C_{SBo} = (OD_\infty - OD_o)/(\alpha L) \quad (7)$$

and

$$C_{SB} = (OD_\infty - OD)/(\alpha L). \quad (8)$$

In the experiments, the concentration of hydroquinone is not measured. Rather, the developer is diluted from a standard stock solution and it is convenient to define a dilution factor as

$$X \equiv C_{Ho}/C_{Hs}. \quad (9)$$

The final film development equations are obtained by combining equations (5) and (7)–(9) with the result

$$OD' = \{1-\exp[-k_r'(Xt)]\}/\{1+(C_{SBo}/C_{So})\exp[-k_r'(Xt)]\} \quad (10a)$$

for reaction I and

$$(1-OD') = \exp[-k_r(Xt)] \quad (10b)$$

for reaction II. In these equations, the normalized optical density is defined as

$$OD' \equiv (OD-OD_o)/(OD_\infty - OD_o). \quad (11)$$

It varies from zero for undeveloped film to a value of unity when all the silver bromide is reduced to metallic silver. Also, lumped reaction rate coefficients have been defined as

$$k_r' \equiv k_I C_{Hs}(C_{SBo}+C_{So})/\lambda \quad (12a)$$

and

$$k_r \equiv k_{II} C_{Hs}/\lambda. \quad (12b)$$

The calibration equation

Now consider the case when diffusion resistance in the developer solution is important. We assume that the accumulation of hydroquinone in the emulsion is so slow that the interfacial uptake of hydroquinone is balanced by its chemical depletion. Representing the rate of uptake by the product of an individual mass transfer coefficient with the difference in hydroquinone concentration between developer solution and emulsion, this balance can be formulated as

$$k_c(C_{Ho}-\lambda C_H) = r_H L \quad (13)$$

where it has been assumed that the volume-to-surface ratio of the emulsion is equivalent to its thickness. As will be demonstrated by well-mixed film development data, the kinetics are adequately represented by reaction II. Assuming also that the ratio of the reactant rates, r_H/r_{SB}, is fixed by a constant stoichiometric coefficient, n, then equations (1b) and (13) can be used to predict C_H

$$C_H = (C_{Ho}/\lambda)/[1+(nLk_{II}/k_c\lambda)C_{SB}]. \quad (14)$$

Combining equations (1b), (3), (9), (12b) and (14) results in a first-order differential equation for C_{SB} which can be integrated with the result

$$C_{SB}/C_{SBo} = \exp[-k_r(Xt) + (nLk_r/k_cC_{Hs})(C_{SBo}-C_{SB})]. \quad (15)$$

This equation can be written in terms of optical density by making use of equations (7), (8) and (11), and then solving for k_c to obtain

$$k_c = \beta(OD')/[k_r(Xt)+\log_e(1-OD')] \quad (16)$$

where a lumped calibration parameter has been defined as

$$\beta \equiv k_{II} n(OD_\infty - OD_o)/\alpha\lambda. \quad (17)$$

Equation (16) relates the mass transfer coefficient at a point on the film to the optical density and the dilution-time product, Xt.

Evaluation and verification

To apply the calibration equation (16), numerical values of the constants k_r and β must be evaluated. A value of k_r can be obtained from an experiment in which the developer is thoroughly mixed such that $k_c \to \infty$ and equation (16) reduces to equation (10b). To determine β, experiments must be carried out in a flow field where the mass transfer coefficient is known from theory. In this work, we employed a rotating disk over which the mass transfer coefficient is constant at a value given by [8]

$$k_c = 0.621 D_H^{2/3} \nu^{-1/6} \omega^{1/2}. \quad (18)$$

Employing 10^{-6} m^2 s^{-1} for ν, and estimating D_H as 8.3×10^{-10} m^2 s^{-1} by applying the Wilke–Chang equation to hydroquinone ion in water [9], equations (16) and (18) can be combined such that

$$(1-OD') = \exp[-k_r(Xt) + (1.82\times10^5)\beta(OD'/\omega^{1/2})]. \quad (19)$$

This equation expresses the relationship between the dependent variable, OD', and the independent vari-

ables, Xt and ω, that are measured in the spinning disk experiment.

A convenient system for verifying the calibration equation is the concentration entrance region of a tube in which liquid flow is fully-developed and laminar. In that case, the local mass transfer coefficient is axisymmetric but varies with axial distance downstream from the leading edge of the film, unlike the spinning disk experiment where k_c is spatially uniform over the surface of the film. At short axial distances, the concentration boundary layer is so thin relative to the momentum boundary layer that the velocity profile of the liquid can be linearized, and the local mass transfer coefficient can be formulated by analogy with the well-known Graetz–Nusselt equation of convective heat transfer [10]. That is,

$$k_c = 2.20(uD_H^2/Rz)^{1/3} \quad (20)$$

when $z < 0.2(uR^2/D_H)$.

METHODS AND MATERIALS

Fine grain black and white film with a speed of 100 ASA (Plus-X, Kodak) was used in all experiments. The unexposed film was stored in a light-tight box. To ensure complete exposure of the emulsion under standardized conditions, the film was removed from the box and held 15 cm from a 100 W incandescent bulb for 20 min just prior to an experiment. The film was then mounted in the test system and contacted for a known period of time with developer solution that was diluted from a stock solution prepared according to the manufacturer's instructions (D-76, Kodak). After removing the film from the test system, the film was rinsed for 30 s (Kodak Stop Bath), fixed for 5 min (Kodak Fixer), rinsed in water for at least 1 h, and submerged in surfactant solution (Photo-flo, Kodak) for 1 min to prevent watermarks during drying.

The opacity of the resulting photographic negatives was quantified by reading OD with a gel chromatogram scanner (Model 620, Bio-rad). A minimum of three scans were made over each piece of film, and edge effects were minimized by excluding the outer 10% of the film surface from the determination of a mean OD. In order to normalize optical density values, OD_0 and OD_∞ values were determined for each new batch of diluted developer and each new film lot. The value of OD_0 was obtained by immersing an exposed piece of film directly in fixer without any development. To obtain OD_∞, a piece of exposed film was immersed in developer solution for 2 days to ensure that all the silver bromide crystals were reduced to silver. A typical value of OD_0 was 0.24 and of OD_∞ was 2.70.

The reaction kinetics of the emulsion were determined by measuring OD changes in well-agitated developer solutions. As previously described by Dasgupta *et al.* [5], 3.5×1.0 cm strips of film were taped to the sides of a beaker containing 1 l of developer solution that was stirred by a high speed impeller. Different film strips were developed for alternative times from 1.25 to 150 min in solutions that were diluted 1/5, 1/10 and 1/40 relative to the developer stock solution.

Evaluation of the calibration equation was performed by employing a spinning disk experiment. A 4.8 cm film disk was dipped in water and placed on the underside of a 4.8 cm diameter stainless steel disk-type spindle mounted in the chuck of rotational viscometer (Model DV-II, Brookfield Instruments). The spindle was then lowered into a beaker containing developer solution. Interfacial tension alone was sufficient to hold the disc in place even after the spindle was rotated. Experiments were performed at: rotational speeds of 5, 10, 20, 50 and 100 rpm; development times from 2.5 to 100 min; and developer dilutions of 1/5, 1/10 and 1/40. The beaker was immersed in a water bath such that the developer solution was thermostated at 25°C. Experiments with the disk submerged 2 cm below the liquid level in a 1-l beaker were duplicated by two different operators. A third set of experiments, with an extension arm added to the spindle so that the disk could be submerged 8 cm below the liquid level in a 4-l beaker, was performed by a third operator.

To further verify the calibration equation, the photographic method was applied inside of a straight tube containing developer solution in laminar flow. The apparatus consisted of an elevated tank containing 14 l of diluted developer that flowed via silicone tubing, first through a rotameter and then through vertical glass tube that emptied into a collection basin. The glass tube had an inner diameter of 0.007 m and a length of 0.3 m. Developer flow was controlled by a screw clamp located downstream of the glass tube, and a constant liquid head was ensured by pumping developer from the collection basin back into the elevated tank. The first 0.24 m of the glass tube served as a velocity calming section, and a 2×6 cm piece of film was inserted into the downstream end of the tube such that it was flush against the inner tube wall. To help it conform to the curvature of the wall, the film was prewound for 24 h on a 0.006 m diameter glass rod before insertion into the tube. Once inside the tube, the exposed film strip was subjected to a constant 3.8×10^{-6} m^3 s^{-1} flow of developer at a dilution of 1/20 for 20 min such that Xt was 1 min. This experiment was replicated four times.

ANALYSIS OF RESULTS

Optical density changes of film in a relatively large volume of developing solution that is well-mixed by a high-speed impeller are due exclusively to chemical reaction kinetics within the emulsion. As the OD' data were uniquely related to Xt (Fig. 1), we conclude that our kinetic data is first-order with respect to the dilution of a controlling reagent (probably the hydro-

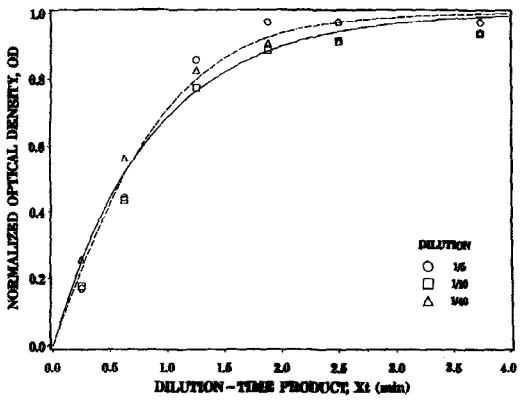

Fig. 1. The kinetics of film development. Optical density of strips of Plus-X 120-format roll film was measured by operator PG in a 1-l volume of well-mixed developer diluted from D-76 stock solution. Since the data (open points) obtained over an eight-fold range of dilutions correlate with the dilution-time product, the kinetics are first-order in the concentration of developer. Alternative least-square regressions of these data to the autocatalytic model I, equation (10a) (interrupted curve), and the noncatalytic model II, equation (10b) (solid curve), had similar summed square errors of 0.0424 and 0.0556, respectively. Therefore, the selection between these two models was based on the estimated parameter values (see text).

quinone anion) in the developer solution. To examine the importance of silver atoms in catalyzing development, OD' data were alternatively regressed to the autocatalytic reaction model I, equation (10a), and the noncatalytic reaction model II, equation (10b). The regressions were performed with a least-square analysis (NLIN, SAS Institute), and the estimated (parameter) $\pm$ (standard error) were $k_r = 0.0193 \pm 0.0010$ s^{-1} for model II and were $k'_r = 0.0282 \pm 0.0048$ s^{-1} and $C_{SBo}/C_{So} = 0.802 \pm 0.564$ for model I. Judging from the standard errors, the value of the rate constant of model II is more precise than that of model I. Moreover, because the latent image consists of very few silver atoms, while the initial concentration of silver bromide is relatively high, C_{SBo}/C_{So} should be much greater than the value estimated from model I. We conclude that equation (10b) more realistically portrays the kinetic data than does equation (10a).

Optical density data from spinning film disks indicated that there were no systematic differences between measurements performed by different operators, or between experiments with the disk submerged in alternative 1-l and a 4-l volumes of developer (Fig. 2). While the OD' vs Xt data generally shifted upward as rotational speed of the disk increased (Fig. 3), the upward shift between 50 and 100 rpm was relatively minor (data not shown). This implies that convective-diffusion was so rapid that the 100 rpm data were controlled by the reaction kinetics within the emulsion. Therefore, the 100 rpm data were regressed to equation (10b), and the resulting $k_r \pm$ (standard error) estimates were 0.0182 ± 0.0015, 0.0183 ± 0.0022 and 0.0175 ± 0.0013 s^{-1} for the three different operators. All of these k_r values obtained from pieces of 8×10-inch Plus-X sheet film used in the spinning disk experiments are within the 95% confidence interval of $0.0213 > k_r > 0.0173$ s^{-1} obtained from pieces of 120-format Plus-X roll film used in the high-speed impeller experiments.

At rotational speeds below 100 rpm, where diffusion limitations existed, the averaged OD data collected by the three operators were analyzed by using a least-square regression to equation (19). The value of k_r was fixed at 0.0180 s^{-1} and β was treated as an adjustable parameter. The resulting regression fits the data quite well at all rotational speeds except 50 rpm, where the measurements were somewhat underpredicted (Fig. 3). The estimate of β from this analysis was $(6.99 \pm 0.15) \times 10^{-6}$ m s^{-1}.

Optical densities in the straight tube experiments were determined at six axial measurement positions from the leading edge of the film (Table 1). The corresponding OD' averaged for four replicated experiments were converted to "observed" k_c by using the calibration equation (16) with the k_r and β values estimated from the spinning disk experiments. A corresponding set of "predicted" k_c values were also obtained by applying equation (20) to all the measurement points. At the last four measurement points, the ratio between the observed and predicted k_c values was in a narrow range of 0.128–0.132, indicating a large but consistent error in the calibration method.

DISCUSSION

When the photographic method was first described [5], mass uptake images were characterized by spatial variations in optical density. The purpose of the present work was to put the photographic method on a more quantitative basis by formulating an equation that converts optical density measurements into liquid phase mass transfer coefficients. The resulting calibration relationship, equation (16), contains two parameters, β and k_r, that depend on a combination of emulsion and developer chemistry.

A classical spinning disk experiment was used to evaluate the calibration equation. In selecting the range of rotation speeds, two conditions were required to satisfy the diffusion theory, equation (18), to which measurements were compared. First, the rotational speed had to be sufficiently fast to minimize the importance of radial diffusion. This is why a minimum speed of 5 rpm was used, even though lower speeds were available on the rotational viscometer. Second, the speed had to be slow enough to avoid flow nonidealities such as secondary circulation patterns and turbulent vortices. At the top speed of the viscometer, 100 rpm, the rate of film development was reaction-limited so that the nature of the flow was immaterial. At 50 rpm, OD' data were somewhat underpredicted by the regressed calibration curve (Fig. 3). This may be due to flow nonidealities that augmented mass transfer. In contrast, the regressed calibration curves

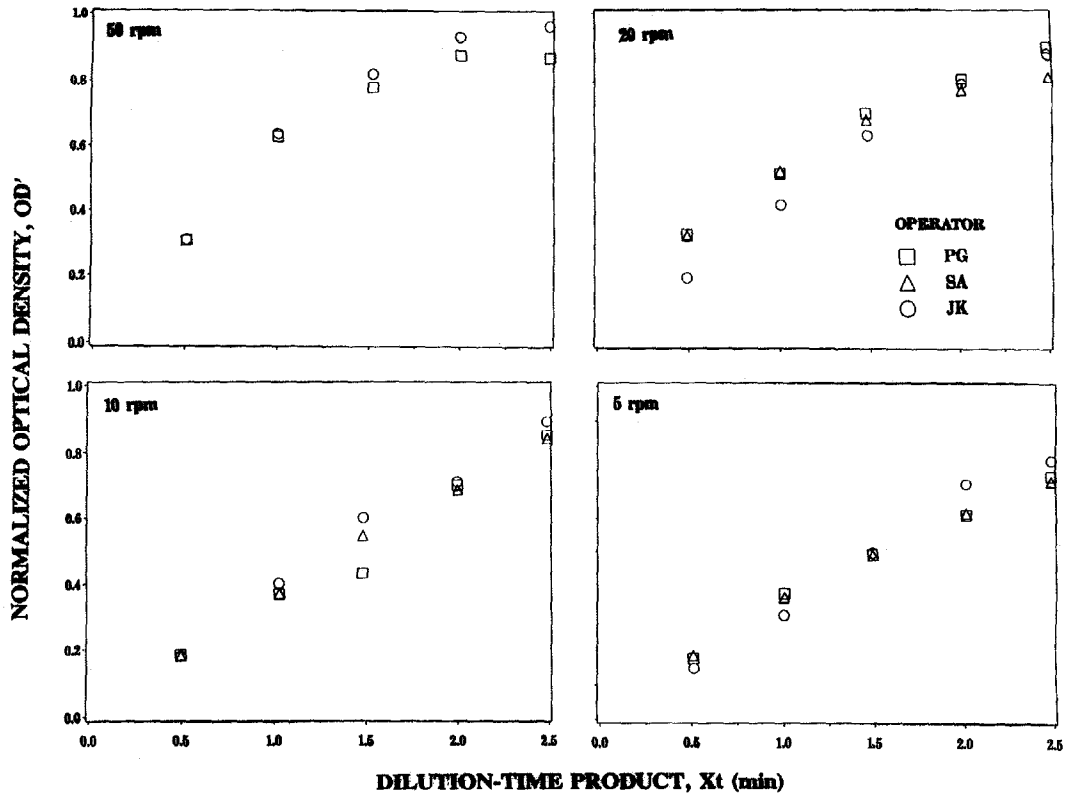

Fig. 2. Spinning disk calibration data. Experiments at a 1/10 dilution of D-76 developer stock solution were replicated using 4.8 cm disks cut from the same box of Plus-X 8 × 10-inch sheet film by three different operators, PG, SA and JK. Each panel shows the results at a fixed rotational speed of the disk between 5 and 50 rpm. Since the data obtained by PG and SA in a 1-l beaker of developer are the same as the data obtained by JK in a 4-l beaker, it can be concluded that boundary effects were unimportant.

fit the data quite well at the lower disk speeds of 5, 10 and 20 rpm.

To verify the calibration, a second independent experiment was conducted in which local k_c values were measured for a developing concentration boundary layer in the entrance region of a tube. Again, two opposing conditions had to be satisfied by the developer flow to ensure consistency with the mass transfer theory, equation (20). First, the flow had to be sufficiently fast that the concentration boundary layer thickness was only a fraction of the momentum boundary layer thickness. For our experiment, where the furthest downstream point was 0.045 m from the leading edge of the film, the inequality condition following equation (20) indicates that the flow must be greater than 10^{-9} m^3 s^{-1}. Second, the flow had to produce a fully-developed laminar velocity profile at the leading edge of the film. Given that there was a 0.24 m long velocity calming section upstream of the film, the maximum acceptable flow was 10^{-5} m^3 s^{-1} [9]. Therefore, the flow of 3.8×10^{-6} m^3 s^{-1} used in the straight tube experiment was within the required upper and lower limits.

There was a large but consistent discrepancy between the k_c that were observed and predicted in the straight tube experiments. Although there is considerable uncertainty in the D_H value used in these computations, the aqueous diffusion coefficient of hydroquinone affects the determination of β and the predicted values of k_c in exactly the same manner (i.e. both are proportional to $D_H^{2/3}$). Therefore, D_H does contribute to the inequality of the observed and predicted k_c values. Another reason for this discrepancy might be an inherent difference in β between the spinning disk and straight tube experiments.

Since β is defined as $k_{ij}n(OD_\infty - OD_o)/\alpha\lambda$, its value should depend solely on the properties of the film emulsion and its interaction with the developer. The same D-76 developer and Plus-X emulsion was used in the spinning disk and the straight tube experiments, but the film formats were different. An 8 × 10-inch sheet film was selected for the former experiment because pieces of this film were sufficiently flat and rigid to conform to the planar surface of the disk, and a 120-format roll film was used in the latter experiments because its inherent curvature and flexibility allowed it to conform to the cylindrical surface inside the tube. It is possible, but not likely, that different values of β were associated with these two film formats.

Fortunately, the use of β can be circumvented by expressing the mass transfer coefficient at each point

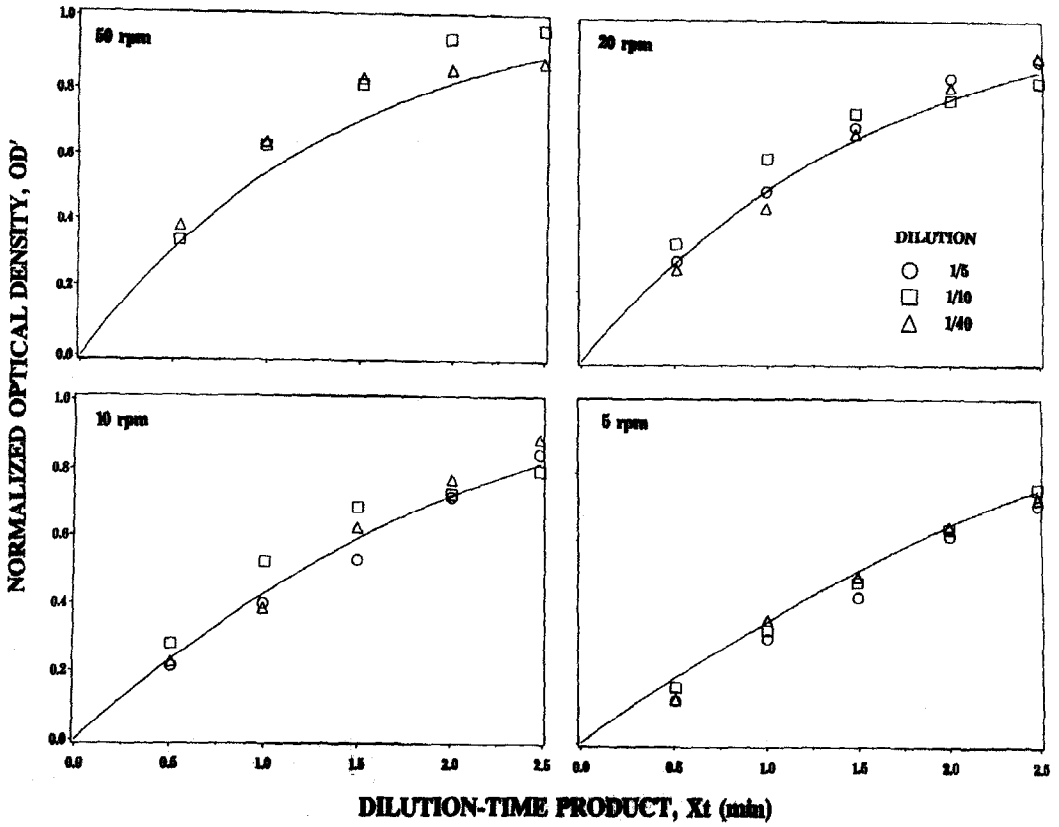

Fig. 3. Regression of spinning disk calibration data. Each data point represents the average value of optical density obtained in three replications of the experiment. The solid curves represent the nonlinear least square regression of equation (16) to the data with a fixed k_r value of 0.0180 s^{-1}, resulting in an estimated β value of 6.99×10^{-6} m s^{-1}.

on a photographic image as a fraction of the value at some reference point. In that case, equation (16) can be reformulated in terms of the normalized mass transfer coefficient

$$k_c/(k_c)_{ref} = (OD'/OD'_{ref})[k_r(Xt) + \log_e(1 - OD'_{ref})]/ [k_r(Xt) + \log_e(1 - OD')]. \quad (21)$$

This equation only depends on the calibration parameter k_r that can be determined by straightforward measurements in mechanically-agitated beakers. To demonstrate the use of equation (21), the data from the straight tube experiment were converted to $k_c/(k_c)_{ref}$ by taking the optical density at $z = 0.035$ m as a reference. According to equation (20), the normalized coefficient should behave according to the equation

$$k_c/(k_c)_{ref} = (z/z_{ref})^{1/3}. \quad (22)$$

As Fig. 4 indicates, the data do closely follow this prediction.

Table 1. Mass transfer in the near-entrance region of a straight tube at a fully-developed laminar flow

Axial distance z [10^{-2} m]	Optical density $OD' \pm$SE	Mass transfer coefficient k_c [10^{-5} m s^{-1}]		
		Observed†	Predicted‡	Ratio
0.0	0.531±0.014	1.150	∞	
1.0	0.407±0.008	0.510	2.72	0.188
1.5	0.309±0.009	0.304	2.38	0.128
2.5	0.275±0.008	0.253	2.01	0.126
3.5	0.258±0.008	0.231	1.79	0.129
4.5	0.248±0.005	0.218	1.65	0.132

†Computed from equation (16) with $\beta = 6.99 \times 10^{-6}$ m s^{-1}, $k_f = 0.0180$ s^{-1} and $Xt = 60$ s.

‡Computed from equation (20) with $D_H = 8.20 \times 10^{-10}$ m^2 s^{-1}, $u = 0.0987$ m s^{-1} and $R = 0.0035$ m.

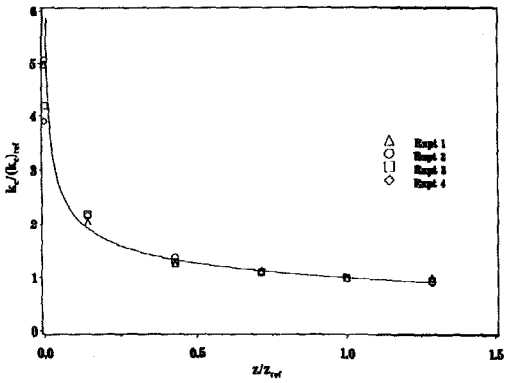

Fig. 4. Axial distribution of the normalized mass transfer coefficient inside a straight tube. The normalized mass transfer coefficient on the ordinate was computed with equation (21) using a k_r value of 0.0180 s^{-1} and a reference optical density at $z_{ref} = 0.035$ m. Developer dilution was 1/20, development time was 20 min, and developer solution flowed at 3.8×10^{-6} m^3 s^{-1}. Each data point represents one experimental trial and the solid curve is the theoretical prediction given by equation (22).

To illustrate how the non-linear nature of equation (21) affects the interpretation of a complex mass transfer patterns, consider the OD' data that were previously measured on the floor of a rectangular flow channel downstream of a backward-facing step [5]. At the largest developer Reynolds number of 13 000, four landmarks are evident in the optical density data (Fig. 5; middle panel): a sharp peak [A] corresponding to a corner eddy is located immediately downstream of the step; a sharp trough [B] corresponding to a large circulating stall is adjacent to the corner eddy; a broad peak [C] corresponds to the region where flow around the stall reattaches to the channel floor and a level value of OD' far downstream of the step [D] implies that the developing boundary layer has reached a constant thickness. Employing this downstream OD' value as a reference, the corresponding distribution of $k_c/(k_c)_{ref}$ indicates that mass transfer in the corner eddy and in the circulating stall is far less important than in the boundary layer reattachment region, where there is a five-fold peak in k_c above its reference value (Fig 5; lower panel). Also, the reattachment peak [C] is narrowed by the application of calibration formula, indicating that the reattachment region as defined by k_c is smaller than is perceived from the OD' data.

The range of applicability of the photographic method can be explored by performing a sensitivity analysis of the calibration equation, equation (16). We define sensitivity as the ratio of a differential change in optical density, $d(OD')$, to a differential fractional change in mass transfer coefficient, $d(k_c)/k_c$. Taking the derivative of equation (16) with respect to k_c indicates that the sensitivity, $k_c d(OD')/d(k_c)$, can be represented as a family of curves of fixed $k_r Xt$ but varying k_c/β (Fig. 6). Along each curve, sensitivity increases rapidly with k_c/β and, after reaching a maximum value, sensitivity gradually decreases. The larger is $k_r Xt$, the larger is the maximum sensitivity but the narrower is the curve. In other words, when selecting experimental Xt conditions, there is a trade-off between the sensitivity and measurement range of the photographic method.

For example, suppose that the maximum tolerable error in k_c is 10% (i.e. $d(k_c)/k_c = 0.1$) and, as suggested by the standard errors in Table 1, the resolution of OD' is 0.01 (i.e. $d(OD') = 0.01$). In that case, the minimum sensitivity would be fixed at $(0.01/0.1) = 0.10$. Of all the curves in Fig. 6, the $k_r Xt = 1$ curve would result in the broadest range of $1.7 > k_c/\beta > 0.2$ over which the sensitivity is always equal to or greater than 0.1. For those curves where $k_r Xt$ is above 1.0, a greater maximum sensitivity could be achieved, but at the expense of a narrower range of k_c/β; for those curves where $k_r Xt$ is below 1.0, a sensitivity of 0.1 cannot be achieved. In the current

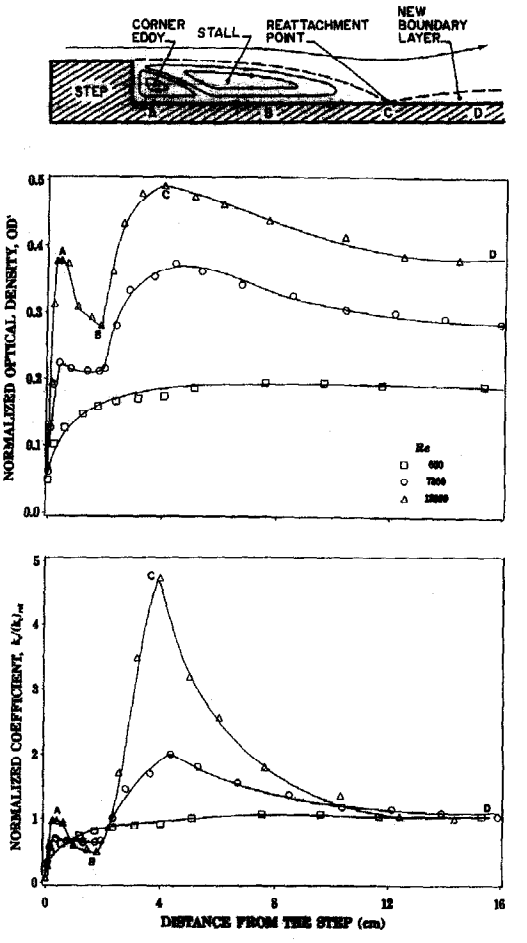

Fig. 5. Axial variations in mass uptake on the floor of an open rectangular channel downstream of a backward facing step. Upper panel: schematic representation of streamline patterns. Middle panel: OD measured downstream of 0.0095 m high step using Plus-X sheet film and D-76 developer at a dilution-time product of 0.6. Lower panel: normalized mass transfer coefficients obtained with equation (21).

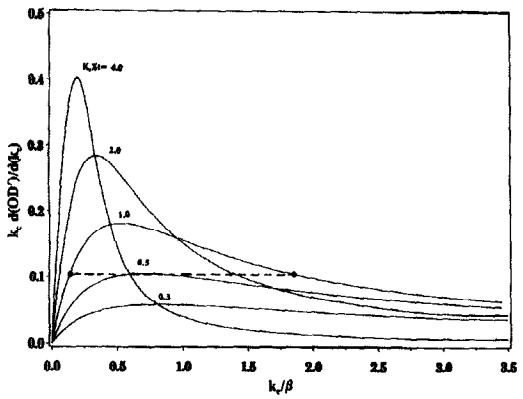

Fig. 6. Sensitivity of the OD'–k_c calibration equation. The derivative of equation (16) is presented as the solid curves. The horizontal interrupted line represents a minimum sensitivity of 0.1 corresponding to a 0.01 change in optical density change per 10% change in the mass transfer coefficient. The intersection of this line with any of the solid curves indicates the range over which k_c/β can be measured with this minimum sensitivity. The broadest range, $1.7 > k_c/\beta > 0.2$, occurs when $k_r Xt = 1$.

study, $k_r = 0.0180\ s^{-1}$ so the optimum $k_r Xt = 1$ corresponds to a dilution-time product of about 1 min.

CONCLUSIONS

A photographic method that uses Plus-X film and D-76 developer can be calibrated with a nonlinear equation that converts optical density to a normalized mass transfer coefficient, and this equation contains only one system parameter, k_r. Since k_r is proportional to the reaction rate in the emulsion, it can be conveniently evaluated in an agitated container where mass transfer limitations have been minimized. Development of a spinning disk of exposed film indicated that the calibration equation accurately accounts for changes in mass transfer due to fluid convection (i.e. changes in the rotational speed of the disk). Moreover, development of an exposed film strip in the entrance region of a straight tube indicated that the calibration equation accurately accounts for spatial changes in mass transfer rate. For a given sensitivity of the optical density to the mass transfer coefficient, there is an optimum choice of the Xt product ensuring that k_c can be adequately resolved over the broadest possible range. Typically, OD' should change by at least 0.01 if we wish to measure the value of k_c within 10%. In that case, the optimum value of Xt is approximately 1.0 min.

Acknowledgements—This work was made possible in part by a research grant from the Chemical Industry Institute of Toxicology to Penn State University.

REFERENCES

1. T. Mizushina, The electrochemical method in transport phenomena. In *Adv. Heat Transfer* (Edited by T. F. Irvine, Jr and J. P. Hartnett), Vol. 7, p. 87. Academic Press, New York (1971).
2. E. M. Sparrow and F. P. Kalejs, Local convective transfer coefficient in a channel downstream of a partially constricted inlet, *Int. J. Heat Mass Transfer* **20**, 1241–1249 (1977).
3. N. Macleod and R. B. Todd, The experimental determination of wall–fluid mass transfer coefficients using plasticized polymer surface coatings, *Int. J. Heat Mass Transfer* **16**, 485–504 (1973).
4. M. R. V. Sahyun, Secrets of photography, *Chemtech* 418–424 (July 1992).
5. A. Dasgupta, P. Guenard, J. S. Ultman, J. S. Kimbell and K. T. Morgan, A photographic method for the visualization of mass uptake patterns in aqueous systems, *Int. J. Heat Mass Transfer* **36**, 453–462 (1993).
6. D. H. O. John, D. H. O. and G. T. J. Field, *Photographic Chemistry*, p. 93. Reinhold, New York (1963).
7. T. H. James, The reduction of silver ions by hydroquinone, *J. Am. Chem. Soc* **61**, 648–652 (1939).
8. V. G. Levich, *Physicochemical Hydrodynamics*, pp. 60–69. Prentice-Hall, Englewood Cliffs, NJ (1962).
9. R. B. Bird, W. E. Stewart and E. N. Lightfoot, *Transport Phenomena*, pp. 47 and 515. Wiley, New York (1960).
10. W. L. McCabe, J. C. Smith, J. C. and P. Harriot, *Unit Operations of Chemical Engineering* (4th Edn), p. 300–301. McGraw-Hill, New York (1985).